

A 5th GENERATION SC SUPERALLOY WITH BALANCED HIGH TEMPERATURE PROPERTIES AND PROCESSABILITY

Akihiro SATO,^{1,2} Hiroshi HARADA,¹ An-Chou YEH,¹ Kyoko KAWAGISHI,¹
Toshiharu KOBAYASHI,¹ Yutaka KOIZUMI,¹ Tadaharu YOKOKAWA,¹ and J-X.ZHANG,^{1,3}

¹High Temperature Materials Center, National Institute for Materials Science (NIMS), Tsukuba, Ibaraki, Japan

²Materials Department, Research Laboratory, IHI Corporation, Yokohama, Japan

³Present Address : Shandong University, Jinan, China

Keywords: 5th Generation Single Crystal Superalloys, Creep, Thermo Mechanical Fatigue, Oxidation, Castability

Abstract

A 5th generation single crystal (SC) superalloy TMS-196 with improved microstructural stability and environmental properties was designed with using NIMS Alloy Design Program and evaluated experimentally. It was found that TMS-196 has a very stable microstructure even after 1000h creep at 1100°C and also very well balanced creep, TMF and environmental properties. TMS-196 also had excellent SC castability; sound cooling blades of up to 300mm long were successfully cast.

Introduction

Alloy development for turbine blade materials with higher temperature capability is crucial in order to improve the thermal efficiency in gas turbine systems for mitigating CO₂ emission. The turbine blade experiences continuous radial loading from the rotation of the turbine in a harsh environment behind the combustor, so high temperature properties of the material, such as creep strength and oxidation resistance can dictate the performance of the gas turbine engine. Through the “High Temperature Materials 21 Project” conducted by the National Institute of Materials Science (NIMS) in Japan, two 5th generation Ni-base single crystal superalloys, TMS-162 and TMS-173 [1] have already been successfully developed to supersede the high temperature creep resistance of all reported Ni-base materials, including the recent 4th generation alloys (EPM-102 and TMS-138) [2, 3].

To design an advanced Ni-base superalloy with improved strength while retaining a balance of properties is a challenging task. Additions of rhenium (Re) and other refractory elements such as tungsten (W) and molybdenum (Mo) have allowed the development of multiple generations of superalloys due to their ability to provide high degrees of solid solution strengthening. However, the addition of refractory elements can also promote the formation of topologically close packed (TCP) phases, which are detrimental to mechanical properties, when the alloy is exposed to elevated temperature environments [4]. As the ability to incorporate high levels of refractory content into these alloys has been limited due to the tendency to result in the formation of TCP phases, additions of platinum group metals (PGMs), especially ruthenium (Ru) additions, become critical to the development of new generations of superalloys by further improving the phase stability [5, 6, 7]. Due to further refractory elements additions becoming possible in conjunction with PGMs additions, the lattice misfit has been increased toward more negative and result in the formation of fine γ/γ' interfacial dislocation network that attribute to a great degree of strengthening [1, 8, 9]. Morphological evolution of the

coherent γ/γ' microstructure into directional formation of the γ' raft perpendicular to the applied stress direction is strongly determined by the magnitude of γ/γ' misfit [10]. Under high temperature and low stress conditions, the rafted microstructure acts as an effective barrier to deformations [7, 8, 11].

TMS-162 and TMS-173 are the first two 5th generation Ni-base single crystal superalloys developed within the “High Temperature Materials 21 Project” of NIMS; both alloys are shown to exhibit excellent creep resistance [1]. Based on the composition of TMS-138, higher Ru content ($\geq 5.0\text{wt}\%$) allows higher Mo and Re additions in TMS-162 and TMS-173, respectively. Additional Mo and Re in conjunction with high Ru concentration for these alloys aim at refining the γ/γ' interfacial dislocation network. So, higher lattice misfit and further solid solution strengthening by Mo and Re (and Ru at lower temperatures, e.g. 800°C [8]), improved phase stability by Ru can all attribute its superiority in creep resistance over previous generations [1, 8]. However, higher Ru and Re content in both low Cr bearing TMS-162 and TMS-173 have resulted in poorer oxidation resistance at elevated temperatures due to vaporization of Ru and Re oxides [12], so a much improved oxidation resistance would be required for their practical applications. During oxidation at temperatures above 700°C, scales of Al₂O₃, Cr₂O₃, NiO, spinel Ni(Cr, Al)₂O₄ can form on advanced superalloys. For alloys upon which scale of Al₂O₃ are formed can exhibit better oxidation resistance, because diffusion transport through Al₂O₃ is slow [13]; formation of continuous Al₂O₃ scale, which is resistant to cracking and spalling, would render the alloy to be more oxidation resistant [14].

In this article, we introduce TMS-196, the flagship alloy in the 5th generation category. TMS-196 has gone through extensive evaluation programmes on its ability to against high temperature creep, thermo mechanical fatigue, phase instability and oxidation. The alloy design process along with test results are summarised and compared with current commercial superalloys.

Alloy Design

The in-house alloy design programme (NIMS-ADP) [15] for high temperature materials development has been established by multiple regression analysis of a large number of experimental data based on statistical valid and systematic experiments; the program is capable in estimating elemental effects and interactions. Its application can assist alloy designers to derive compositions by manipulating parameters, such as γ' volume fraction, lattice misfit, alloy density, phase stability and creep rupture life.

Table I. Some examples of 2nd, 3rd and 4th generations of superalloys compositions (wt%), associated with alloy density ρ (g/cm³) estimated by NIMS alloy design program.

| Alloy Generations | | Cr | Co | Mo | W | Al | Ti | Ta | Hf | Re | Ru | ρ |
|-------------------|--------------|-----|------|-----|-----|------|-----|-----|------|-----|-----|--------|
| 2 nd | CMSX-4 | 6.5 | 9.0 | 0.6 | 6.0 | 5.6 | 1.0 | 6.5 | 0.1 | 3.0 | - | 8.70 |
| | PWA1484 | 5.0 | 10.0 | 2.0 | 6.0 | 5.6 | - | 9.0 | 0.1 | 3.0 | - | 8.95 |
| | Rene' N5 | 7.0 | 8.0 | 2.0 | 5.0 | 6.2 | - | 7.0 | 0.2 | 3.0 | - | 8.63 |
| 3 rd | Rene' N6 | 4.2 | 12.5 | 1.4 | 6.0 | 5.75 | - | 7.2 | 0.15 | 5.4 | - | 8.98 |
| | CMSX-10 | 2.0 | 3.0 | 0.4 | 5.0 | 5.7 | 0.2 | 8.0 | 0.03 | 6.0 | - | 9.05 |
| | TMS-75 | 3.0 | 12.0 | 2.0 | 6.0 | 6.0 | - | 6.0 | 0.1 | 5.0 | - | 8.89 |
| 4 th | MX-4/PWA1497 | 2.0 | 16.5 | 2.0 | 6.0 | 5.6 | - | 8.3 | 0.15 | 6.0 | 3.0 | 9.20 |
| | MC-NG | 4.0 | 0 | 1.0 | 5.0 | 6.0 | 0.5 | 5.0 | 0.1 | 4.0 | 4.0 | 8.75 |
| | TMS-138 | 3.2 | 5.8 | 2.9 | 5.9 | 5.8 | - | 5.6 | 0.1 | 5.0 | 2.0 | 8.95 |
| | TMS-138A | 3.2 | 5.8 | 2.9 | 5.6 | 5.7 | - | 5.6 | 0.1 | 5.8 | 3.6 | 9.01 |
| 5 th | TMS-162 | 3.0 | 5.8 | 3.9 | 5.8 | 5.8 | - | 5.6 | 0.1 | 4.9 | 6.0 | 9.04 |
| | TMS-173 | 3.0 | 5.6 | 2.8 | 5.6 | 5.6 | - | 5.6 | 0.1 | 6.9 | 5.0 | 9.11 |
| | TMS-196 | 4.6 | 5.6 | 2.4 | 5.0 | 5.6 | - | 5.6 | 0.1 | 6.4 | 5.0 | 9.01 |

Compositions of recent NIMS superalloys and some other commercial alloys are summarised in Table I. To improve the oxidation resistance of TMS-162 and TMS-173, Cr content in TMS-196 was increased to 4.6wt% [16]. Cr additions could promote the formation of protective Al₂O₃ scale against oxidation [17]. By calculations based on NIMS-ADP, the additional 1.6wt% Cr with fine adjustment of Mo, W and Re concentrations can retain the γ' volume fraction and lattice misfit of TMS-173 in TMS-196.

Casting and Heat Treatment Processes

The master ingots of TMS-196 were vacuum induction melted at Ishikawajima Master Metal (IMM), Japan. Evaluations on high temperature creep, TMF and oxidation of TMS-196 were carried out with single crystal bars (10mm diameter and 130mm length) fabricated at NIMS using conventional withdrawing technique typical condition being 200mm/hour withdraw rate for 8 bars in a mould with pigtail grain selectors.

As-cast bars of TMS-196 were subjected to solution heat treatment at 1340°C for 10hours. To determine the optimal primary ageing temperature, as-solutioned samples were heat-treated for 4hours at 1100°C, 1125°C, 1150°C, 1175°C and 1200°C, followed by secondary ageing at 870°C for 16hours. Microstructures were examined for chemical homogeneity, γ/γ' morphology and volume fractions. As the ageing temperature increased, the average size of γ' also increased. 1100°C primary ageing resulted in regular and cuboidal γ' structures (64% γ' volume fraction with γ' size \sim 0.2 μ m), Figure 1(a). However, some tendency of losing coherency between γ and γ' was detected in samples aged at higher temperatures, Figure 1(b). Samples aged at 1175°C and 1200°C exhibited severe

widening of the γ channels and coarse γ' particles in the dendrite areas.

Specimens subjected to different primary ageings were creep tested at temperatures between 800°C and 1100°C, results indicated that TMS-196 aged at 1100°C possessed the optimal γ/γ' microstructure and performed best against creep. So, the 1100°C / 4hours primary ageing was chosen as the standard process condition for samples analyzed in the following sections.

Mechanical Properties

Bars of as-cast single crystal TMS-196 were solution-treated at 1340°C for 10hours followed by a primary age for 4 hours at 1100°C and a secondary age for 16 hours at 870°C. Samples of orientations within 9 degrees of the <001> were chosen and machined into standard creep specimens and TMF samples for testing.

Creep Behaviours

A wide range of temperature and stress conditions was covered to creep test TMS-196, and creep data were used to plot the Larson-Miller diagram along with other alloys for comparisons, Figure 2. TMS-196 clearly exhibited superior creep strength over current commercial superalloys - Rene'N5, CMSX-4 and CMSX-10; the plot indicated an impressive 47°C improvement over CMSX-4 at 1000°C/245MPa. Since TMS-196 was designed for maximum strength with acceptable phase stability and oxidation resistance, this alloy possessed high negative misfit, especially at elevated temperatures. The measured misfit of TMS-196 at 1100°C is -0.39. This high negative misfit promoted formations of raft γ/γ' microstructure during creep at

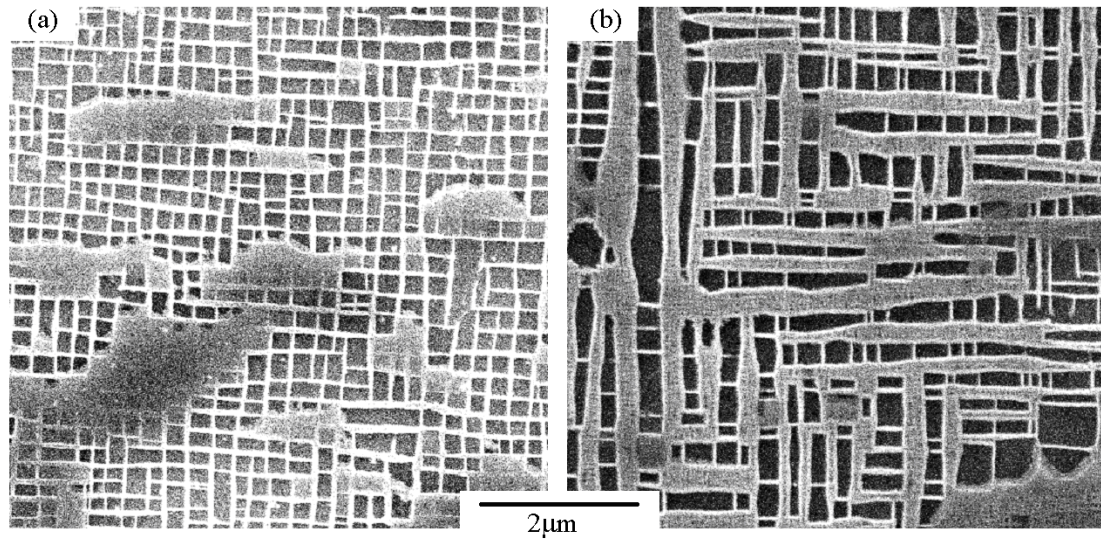


Figure 1. SEM images of γ/γ' microstructures taken at the dendrite cores, solutioned TMS-196 after (a) 1100°C primary ageing for 4 hours, γ/γ' are regular with γ' size $\sim 0.2\mu\text{m}$ (b) 1175°C primary ageing for 4 hours, incoherent γ/γ' and severe widening of γ channels. (γ is the brighter phase and γ' is the darker phase).

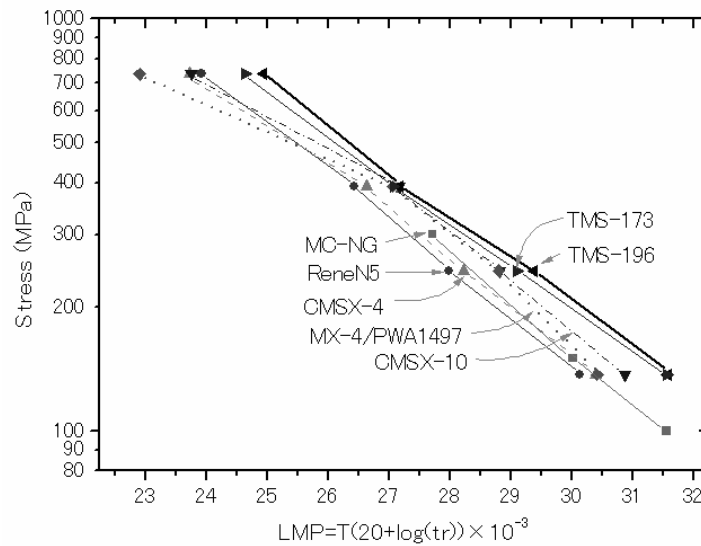


Figure 2. Larson-Miller plot shows significant creep advantage of TMS-196 over other commercial or experimental alloys.

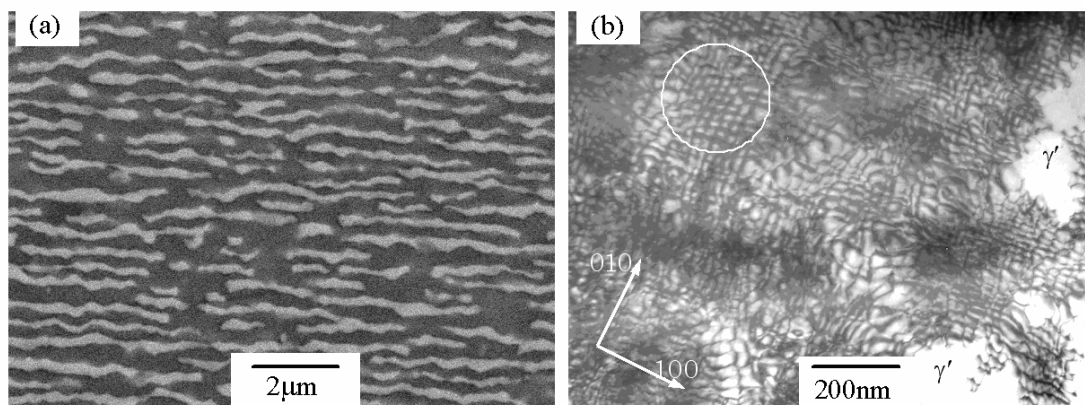


Figure 3. Microstructures of TMS-196 after creep at 1000°C/245MPa. (a) SEM images shows formation of raft structure. (b) TEM bright field image shows the formation of fine γ/γ' interfacial dislocation network (an example is shown in the circled region).

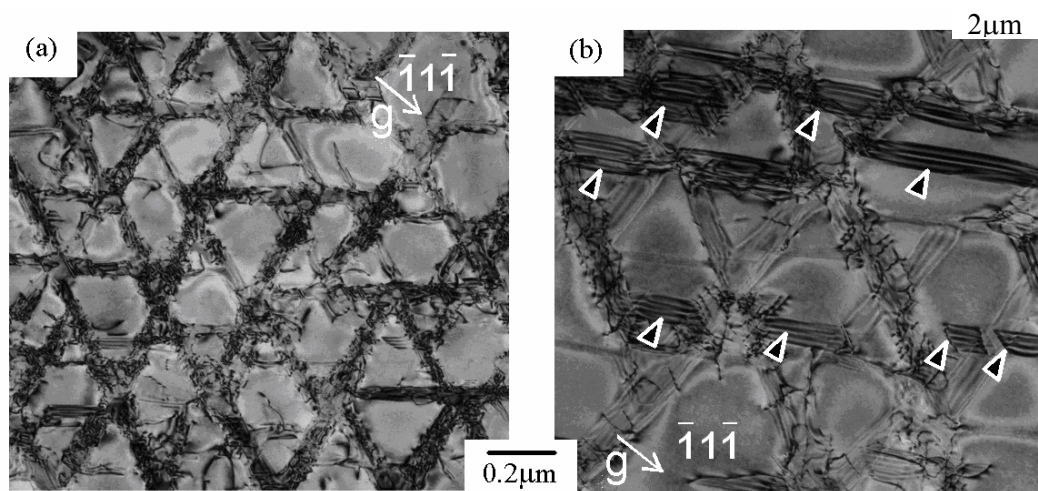


Figure 4. (a) TEM bright field image of TMS-196 interrupted creep until 1% strain at 800°C/735MPa. Time taken to reach 1% creep strain was 727hours, the TEM micrograph indicates dislocations were mainly confined at the γ/γ' interface. (b) For a typical 3rd generation alloy, TMS-75, 1% creep strain at 800°C/735MPa only took less than an hour and resulted many super stacking faults (indicated by arrows) in γ' .

temperatures $\geq 900^\circ\text{C}$, Figure 3(a) and the fine interfacial dislocation network, Figure 3(b). Both features attributed to the excellent creep resistance of this alloy. During creep at 800°C/735MPa, the γ/γ' of TMS-196 appeared to be very resistant to deformation, as dislocations were mainly confined at the γ/γ' interfaces, Figure 4(a). In contrast, in a third generation alloy crept in the same condition, γ' sheared by super-lattice stacking faults could be observed throughout the microstructure, Figure 4(b).

Thermo-Mechanical Fatigue (TMF) Property

TMF tests were performed on test pieces in air to failure on a hydraulic-servo system fatigue machine (MTS type 810). Figure 5 shows schematic drawings of the TMF experimental procedure. The temperature was varied between 400°C and 900°C, which corresponded to the points of maximum tensile and compressive stresses, respectively (i.e. out-of-phase). The strain was controlled with a total range $\epsilon_t = 1.28\%$ ($\pm 0.64\%$), and a triangular waveform was adopted with a frequency of 6 minutes per cycle with 1hour holding time in between at 900°C.

This TMF test cycles was designed to simulate thermal and stress changes experienced in the actual turbine blade during service.

The results of TMF tests were summarised in Table II. TMS-196 exhibited better TMF property than other alloys. Especially the number of cycles to failure for TMS-196 was over two times the cycles of Rene'N5, Table II. As the TMF cycles increased, magnitude of stress relaxation also increased. However, stress relaxation for TMS-196 was relatively small in comparison to the other two alloys, and it resulted in much less plastic deformations.

Zhang et al. [18] show that deformation twins can be seen by a optical microscope and a SEM and suggest that the deformation twin during TMF influence TMF life. The microstructures of TMF ruptured TMS-196 exhibited homogeneous distribution of deformation twins, which could be attributed to an alloy system with low stacking fault energy, Figure 6. This was in contrast to the large deformation twins distributed heterogeneously as observed in some 3rd generation alloys [18].

High Temperature Phase Instability

Thermodynamically stable TCP phases can form in Ni-based single crystal superalloys after exposures at high temperatures. The precipitation is more pronounced during elevated temperature creep due to the increase in the number of stress induced vacancies and accelerated diffusion rates, the associated formation of γ' envelope surrounding the TCP phases can result in localised stress concentrations at the junction of TCP linkage during creep [4]. The presence of brittle TCP precipitates in the microstructure is detrimental to mechanical properties, because its absorption of critical elements (Re, W, Mo and Cr) from the matrix and its disruption on the morphology of the rafted and unrafted microstructures can lead to the onset of tertiary creep. So, it is critical to hinder the phase instability associated with the formation of TCP precipitates for optimal creep performance. TMS-196 contains 5.0wt% Ru to counteract the tendency for phase instability attributed by high Re, Mo and W content.

Samples of TMS-196 were capsulated and then subjected to isothermal exposures at 1100°C for various length of time up to 3000hours, microstructures along the (100) plane were examined for presence of TCP phases and the onset of those precipitates were used as indicators for comparisons with current commercial superalloys. Although the number of TCP phases increased with superalloys. Although the number of For the current commercial superalloy, CMSX-10, a 1% area fraction of TCP precipitates plus γ' envelopes was detected after 100hours exposure at 1100°C [19]. In comparison, after 600hours exposure at 1100°C, less than 0.5 % area fraction of TCP phases was measured in the microstructure of TMS-196, solution-treatment could attribute to greater creep resistance.

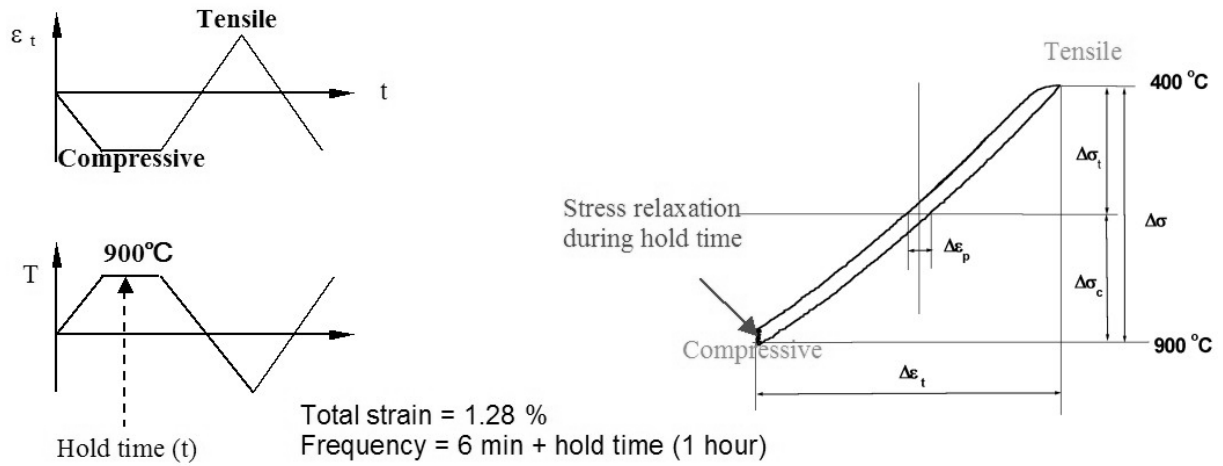


Figure 5. Thermo Mechanical Fatigue test cycle.

Table II. TMF test results of TMS-196 in comparisons with other alloys

| Alloy | Cycles to Failure, Nf | Stress Relaxation (MPa) – (the smaller, the better) | | |
|----------|-----------------------|---|--------|------|
| | | N=1 | N=Nf/2 | N=Nf |
| Rene'N5 | 92 | 150 | 140 | 290 |
| TMS-138A | 124 | 140 | 60 | 140 |
| TMS-196 | 198 | 20 | 10 | 70 |

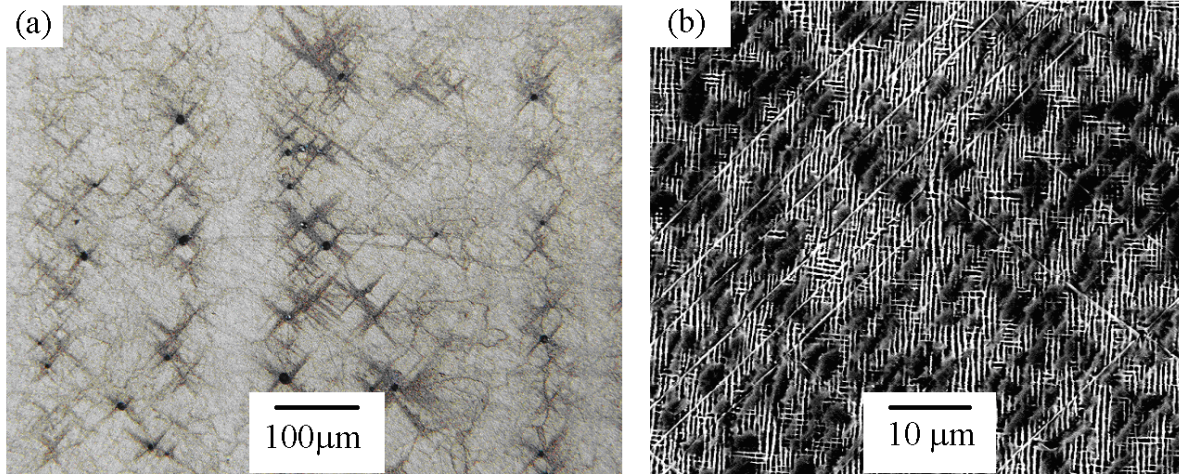


Figure 6. Microstructures of TMS-196 after thermo-mechanical fatigue tests to rupture. (a) The optical image showed homogeneous twinning traces throughout the microstructure. (b) SEM image with higher magnification showed high density of deformation twins.

Oxidation Resistance

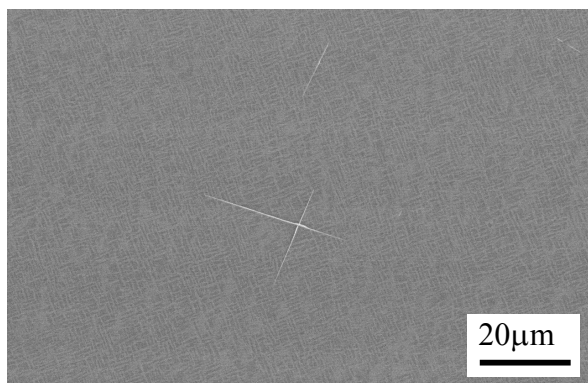


Figure 7. Microstructural changes in TMS-196 after 600hours at 1100°C in dendrite core region.

One hour cyclic oxidation tests were performed at 1100°C in air, and the weight change of each sample was measured by analytical balance. Other commercial single crystal superalloys were also tested for comparative study. PWA1484, CMSX-4 and Rene'N5 compositions were cast and heat treated at NIMS by same procedure as TMS-196. The weight changes of TMS-173, TMS-196, CMSX-4 and Rene'N5 during 50 cycles of 1hour cyclic oxidation tests were shown in Figure 8. Large weight gain during the first 5 cycles followed by severe weight loss was observed in TMS-173. On the other hand, TMS-196 exhibited good resistance to oxidation. The weight change behaviours of TMS-196 was almost identical to that of Rene'N5 and slightly more severe than CMSX-4 and PWA1484.

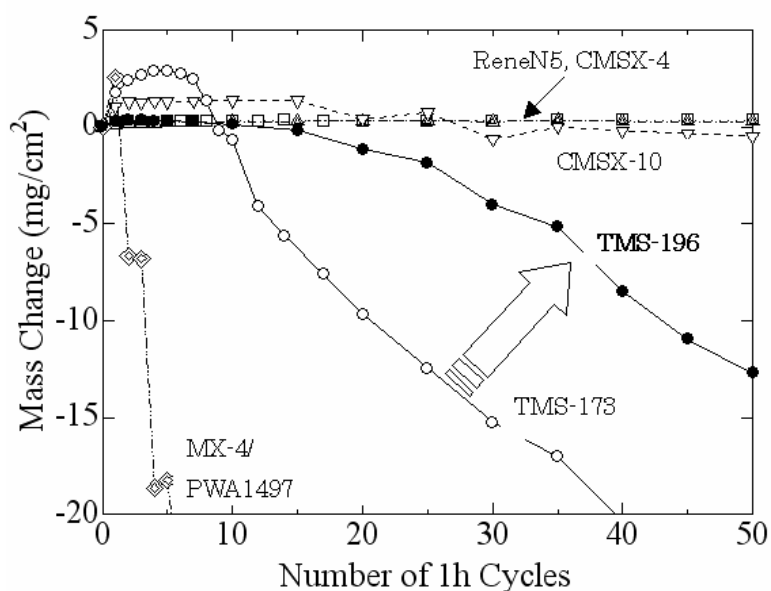


Figure 8. Cyclic oxidation test results at 1100°C.

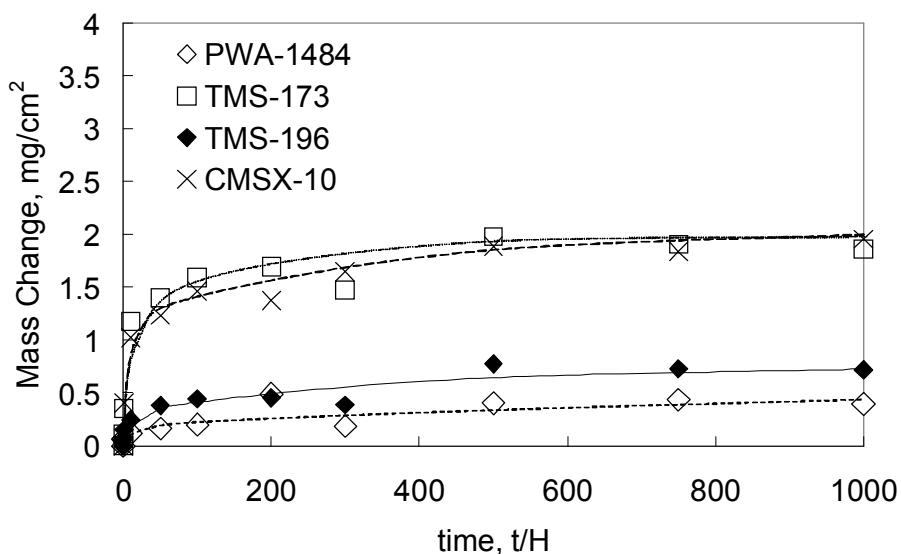


Figure 9. Isothermal oxidation test results at 900°C.

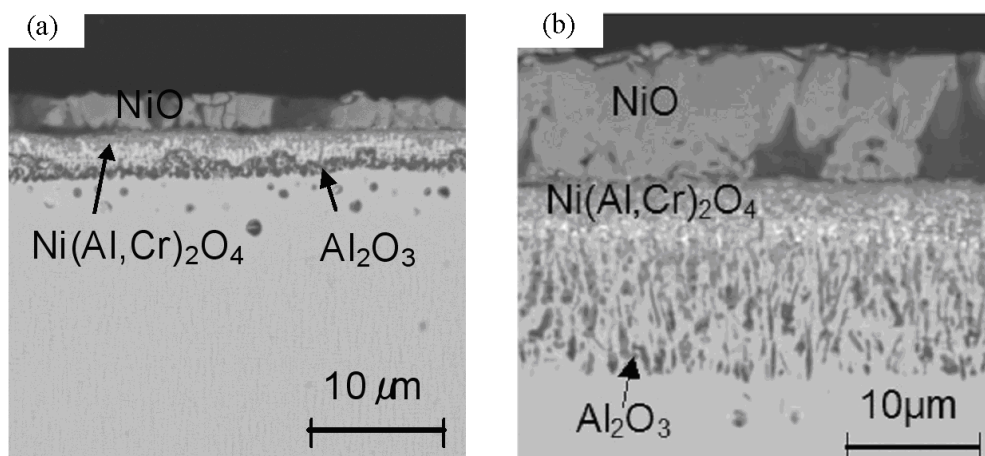


Figure 10. SEM micrographs of (a) TMS-196 and (b) TMS-173 after 1 hour oxidation at 1100°C. TMS-196 exhibited continuous Al_2O_3 scale on the surface.

Mass changes were also measured on samples of PWA1484, TMS-173, CMSX-10 and TMS-196 after isothermal exposure at 900°C for various amount of time up to 1000 hours. Results again indicated that TMS-196 exhibited strong oxidation resistance, similar to that of PWA-1484 and much better than TMS-173 and CMSX-10, Figure 9.

Cross sectional SEM images of TMS-196 and TMS-173 after 1 hour cycle test at 1100°C were shown in Figure 10 (a) and (b). The average oxide layer thickness of TMS-173 and TMS-196 were measured to be around 26 μm and 7 μm, respectively. The oxide layer in both alloy consisted of NiO, $\text{Ni}(\text{Cr},\text{Al})_2\text{O}_4$ and Al_2O_3 . Particle-like Al_2O_3 layer was observed in TMS-173, and continuous Al_2O_3 layer was observed in TMS-196 attributing better oxidation resistance.

Castability

TMS-196 has been successfully cast to actual single crystal cooling blades of about 115mm and 300mm lengths at a Japanese casting house in a context of "1700°C Combined Cycle Gas Turbine Project" run by Mitsubishi Heavy Industries and NIMS, as shown in Figure 11. The casting trials showed that there was no freckle defect in the blades and the casting yield of TMS-196 seemed to be as high as that of conventional 2nd generation single crystal superalloys.



Figure 11. TMS-196 casting trial to a hollow single crystal turbine blade for a land-based gas turbine.

Summary

The present article has demonstrated that TMS-196 is a strong candidate alloy as turbine blade materials for applications in future jet engines. This alloy possesses a balance of excellent properties, which are desired by gas turbine and aero engine manufacturers in order to further enhance their efficiencies. TMS-196 with a density of 9.01 g/cm³ possesses significant advantage in elevated temperature properties over the current commercial superalloys, such as CMSX-4, CMSX-10, PWA1484 and Rene'N5. The highlights of alloy design concept for the 5th generation Ni-base single crystal superalloy (TMS-196) and its evaluations are as followings:

- By increasing the Ru content to further extend the phase stability limit, manipulations in refractory elements content allow the development of the 5th generation superalloys. TMS-196 contains higher Ru, Re and Cr over the 4th generation alloys
- High misfit of TMS-196 has attributed formation of raft structure and finer interfacial dislocation network to inhibit dislocation motions and result excellent creep resistance. A 47°C improvement on creep over CMSX-4 at 1000°C has been achieved.
- TMS-196 exhibits more than two times the thermo mechanical fatigue life cycles of Rene'N5.
- TMS-196 possesses superior phase stability than current commercial alloy, CMSX-10.
- Moderate amount of Cr in TMS-196 allows the alloy to retain acceptable oxidation resistance, which is similar to that of Rene'N5.
- The castability of TMS-196 appears to be similar to that of the 2nd generation alloys.

Acknowledgements

The authors would like to thank also to Mr. S. Nakazawa for his support with the creep experiments.

References

1. Y. Koizumi, T. Kobayashi, T. Yokokawa, Z. Jianxin, M. Osawa, H. Harada, Y. Aoki and M. Arai, "Development of Next-Generation Ni-Base Single Crystal Superalloys", *Superalloys 2004*, (TMS, 2004), 35-43.

2. .S. Walston, A. Cetel, R. MacKay , K. O'Hara, D. Duhl and R. Dreshfield, "Joint Development of a Fourth Generation Single Crystal Superalloy", *Superalloys 2004*, (TMS, 2004), 15-24.
3. T. Kobayashi, Y. Koizumi, T. Yokokawa, and H. Harada, "Development of a 4th Generation DS Superalloy", *Journal of the Japan Institute of Metals*, **66**, (2002), 897-900.
4. T. Hino, Y. Yoshioka, K. Nagata, H. Kashiwaya, T. Kobayashi, Y. Koizumi, H. Harada, and T. Yamagata. "Design of a high Re containing single crystal superalloys for industrial gas turbines", *Proc. 6th Liege Conference on Materials for Advanced Power Engineering*, (COST, 1998), 1129-1137.
5. K.S. O'Hara, W.S. Walston, E.W. Ross, and R. Darolia. in. Nickel base superalloy and article. USA General Electric Co. Patent: US5482789. 9 Jan. 1996.
6. T. Kobayashi, Y. Koizumi, H. Harada and T. Yamagata. "Design of high Re containing single crystal superalloys with balanced intermediate and high temperature creep strengths", *Proc. 4th int'l Charles Parsons turbine conference*, (The institute of materials, 1997), 766-773.
7. T. Yokokawa, M. Osawa, K. Nishida, T. Kobayashi, Y. Koizumi, and H. Harada, " Partitioning behavior of platinum group metals on the gamma and gamma ' phases of Ni-base superalloys at high temperatures", *Scripta Materialia*, **49**, (2003), 1041-1046.
8. J.X. Zhang, T. Murakumo, H. Harada, Y. Koizumi, and T. Kobayashi. "Creep Deformation Mechanism in Some Modern Single-Crystal Superalloys", *Superalloys2004.*, (TMS, 2004), 189-195.
9. J. X. Zhang, T. Murakumo, Y. Koizumi, T. Kobayashi, H. Harada and S. Masaki Jr., "Interfacial Dislocation Networks Strengthening a Fourth-Generation Single-Crystal TMS-138 Superalloy", *Metall. Mater. Trans. A*, **33**, (12) (2002), 3741-3746.
10. T. Ichitsubo, D. Koumoto, M. Hirao, K. Tanaka, M. Osawa, T. Yokogawa, and H. Harada, "Elastic anisotropy of rafted Ni-base superalloy at high temperatures" *Acta Materialia* ,**51**, (2003), 4033-4044.
11. A.C. Yeh, C.M.F. Rae, and S. Tin, "High Temperature Creep of Ru-Bearing Ni-Base Single Crystal Superalloys" *Superalloys2004*, (TMS, 2004), 677-685.
12. K. Kawagishi, H. Harada, A. Sato, A. Sato, and T. Kobayashi, "Oxidation Properties of Fourth Generation Single-Crystal Nickel-Based Superalloys" *JOM*, **58**, (2006), 43-46.
13. J.L. Smialek and G.H. Meier, *Superalloys II*. (New York, NY: John Wiley & Sons, 1987)
14. F.S. Pettit and G.W. Goward, " High temperature corrosion and use. of coatings for protection", *Metallurgical Treatises*, (1981), 603-619.
15. H. Harada, K. Ohno, T. Yamagata, T. Yokokawa, and M. Yamazaki, "Phase Calculation and Its Use in Alloy Design Program for Nickel-Base Superalloys", *Superalloys1988*. (TMS, 1988), 733-742.
16. A. Sato, H. Harada, T. Kobayashi, T. Murakumo, J.X. Zhang, and T. Yokokawa," A 5th Generation Ni-Base Single Crystal Superalloy Designed for the Combination of Excellent Oxidation Resistance and Creep Strength at Elevated Temperatures", *Japan Institute of Metals*, **70**, (2006), 196-199..
17. C.S. Giggins and F.S. Pettit, "Oxidation of Ni-Cr-Al Alloys between 1000C and 1200C", *J. Electrochem. Soc.*, **118**, (1971), 1782-1790.
18. J.X. Zhang, Y. Ro, H. Zhou, and H. Harada, "Deformation twins and failure due to thermo-mechanical cycling in TMS-75 superalloy", *Scripta Materialia*, **54**, (2006). 655-660.
19. G.L. Erickson, "The Development and Application of CMSX-10", *Superalloys1996*, (TMS, 1996), 35-44.